Sirtoli, D., Lura, P., Marchi, M. and Tortelli, S., 2018. Drying and Autogenous Shrinkage Evolution of a Blended CSA-Portland Cement Concrete. Special Publication, 326, pp.30-1. https://doi.org/10.1016/j.cemconcomp.2019.02.006

# Shrinkage and creep of high-performance concrete based on calcium sulfoaluminate cement

Davide Sirtoli[1], Mateusz Wyrzykowski[2], Paolo Riva[1], Sergio Tortelli[3], Maurizio Marchi[3], Pietro Lura[2,4]

1. Dept. of Engineering, Univ. of Bergamo, Viale Marconi 5, 24044 Dalmine, Italy
2. Empa, Swiss Federal Laboratories for Materials Science and Technology, Überlandstrasse 129, 8600 Dübendorf, Switzerland
3. Italcementi – Heidelberg cement group
4. Institute for Building Materials (IfB), ETH Zurich, 8092 Zurich, Switzerland

## ABSTRACT

Calcium sulfoaluminate (CSA) cements can be used in concrete as an alternative binder, as full or partial replacement of Portland cement. This enables reducing $CO_2$ emissions from cement production and offers other advantages, e.g. fast gain of mechanical properties. However, very little data is available on the behaviour of concretes with CSA binders, in particular on their creep and shrinkage. This paper presents a study on volume stability of high-performance concretes with CSA binder, blended with, or completely replacing, Portland-limestone cement. Shrinkage and creep in both autogenous and drying conditions were measured from 1 day until 1 year. The experimental results were compared with the empirical models Model Code 2010 and ACI 209.R-92. The results indicate that standard models originally developed for Portland cement concretes do not allow to address the pronounced differences between the Portland and CSA-based concretes, since their main input data are merely based on compressive strength.

**Keywords:** Calcium sulfoaluminate cement, high performance concrete, shrinkage, creep, model code.

## 1. INTRODUCTION

Calcium sulfoaluminate cement (CSA) represents an ecological alternative to Portland cement (PC) due to its reduced $CO_2$ emissions during production [1]. The main constituent of CSA clinker is ye'elimite ($C_4A_3\bar{S}$), in combination with other phases like belite ($C_2S$), ferrite ($C_4AF$), mayenite ($C_{12}A_7$) and anhydrite, depending on the raw materials used [2,3]. Usually, around 20% by mass of calcium sulphate is added to CSA clinker to regulate the setting time, the strength development and the volume stability of the cementitious matrix [2], creating a binary system. The main hydration product is ettringite (AFt), which is formed from the reaction of ye'elimite, lime and sulphates, the latter of great importance for their kinetics [4]. A possible alternative to the pure system is represented by blends of CSA and PC. In these blends, the hydration process is governed by the calcium sulfoaluminate cement in the first days, while the Portland cement reacts later [5]. The precipitation of AFt during early-age hydration is mainly responsible for the development of the material properties, like fast setting, rapid hardening [6] or expansion for shrinkage compensation [6,7]. After the rapid CSA reaction in the first days, the PC starts to react, leading to long-term performance improvement [8].

In the 1970s, the People's Republic of China started a large research program on calcium sulfoaluminate and calcium sulfoaluminate belite cements aiming to improve the knowledge about this class of binders. Twenty years of experience in production (albeit with low amounts of CSA produced yearly) and use led to standardization both of the cement and of concrete mixture compositions [9]. The main outcome of this program was the need to focus on the rapid-hardening behavior of these materials, which is its most useful and powerful characteristic, though it is also the most complex aspect to control. The Chinese experience is the only example so far of a research program of such dimensions and complexity on CSA. In recent years, significant steps forward in the basic understanding of CSA's chemical and physical properties were accomplished. However, the practical use of CSA is still limited to niche products, e.g., as expansive agent to compensate shrinkage of PC concrete [10–12], in the production of self-levelling screeds [13], as sealing mortar for road works [14] and as tile adhesive [15].

While the dimensional stability of calcium sulfoaluminate systems under water cured conditions has been studied (e.g., [16]), its application in structural concrete with other exposure conditions of the surface should be examined. In particular, sealed conditions in the first days of hardening (representative for the period before demolding) followed by drying conditions at later ages (after demolding) [17] need to be investigated. Due to the initial fast reaction of CSA systems, particular attention is required in the first stage, when the material is under autogenous conditions [18]. This is of great importance especially when the water-to-cement ratio (w/c) is lower than the minimum value required by the stoichiometry of the cement hydration reaction [19]. This value represents the limit between systems that may theoretically achieve full hydration and systems where a portion of the

cement remains unreacted due to insufficient amount of water for hydration, causing self-desiccation. This w/c is around 0.40-0.42 for PC and depending on the amount of added calcium sulphate up to 0.78 for pure ye'elimite [3]. For a specific CSA, a value of 0.75 was recently measured [20]. Considerable pore fluid pressures are generated in a system that undergoes self-desiccation, leading to autogenous deformation and build-up of self-induced stresses that must be limited to avoid cracking [21,22]. At the same time, creep and relaxation play an important role in both deformation and cracking behavior of the new systems; to the authors' best knowledge, very limited data has been published so far on this aspect for the CSA-based systems.

Building up on a previous publication that focused mainly on the mechanical properties [23,24], this study has the aim of investigating the deformation behavior of concrete systems containing either pure CSA or a blend with PC, in terms of shrinkage and creep evolution in both autogenous and drying conditions. This study covers the stage after concrete demolding and up to 1 year of age, underlining the possible interactions between the two investigated conditions on the stability of the matrix, with and without external mechanical loads. The experimental results are compared to shrinkage and creep predictions according to Model Code 2010 [25] and ACI 209.R-92 (1992) [26] to highlight the differences with PC-based concrete and assess whether new predictive models need to be developed for these systems.

## 2. MATERIALS AND METHODS

### 2.1. Materials

Three concrete mixtures made with 1) pure CSA, 2) a Portland-limestone cement, CEM II A-LL 42.5 R, and 3) a blend of the two (50/50 ratio by mass) were considered for this study; in the following, they will be labelled as CCSA, CPC and CMIX, respectively. The CSA had as main components (by mass %, measured by XRD): ye'elimite 53.0, anhydrite 18.7, bredigite 10.7, $C_2S$ 7.7. The Portland-limestone cement was chosen for the stabilization effect of the calcium carbonate on the ettringite that will form during hydration [15,27,28]. Its phase composition (by mass %, measured by XRD) was: $C_3S$ 55.4, $C_2S$ 9.3, $C_3A$ 3.3, $C_4AF$ 9.7 and calcite 12.4.

The mix design is based on the mixtures developed for a previous study [8], which were designed with the target of reaching the same 28-day strength class C50/60 and at least 160 mm slump after 45 minutes from water addition. This approach was chosen because it would be the practical approach followed by a concrete producer. In order to reach the same strength class, the w/c and the amount of cement in the three mixtures were different (see Table 1), while the total amount of aggregates was similar (small adjustments were however necessary for workability reasons). The paste volume was almost identical in the three mixtures. The mixtures were prepared with siliceous coarse rounded aggregate (maximum diameter 20 mm) and river sand conforming to the EN 12620 standard. A

polycarboxylate-based superplasticizer (SP) in liquid form was used in all concretes. Compared to the original mix design used in [8], the superplasticizer amount was lower thanks to the more efficient concrete mixer (see below) used during this project. Citric acid as hydration retarder and lithium carbonate as set inductor, both in powder form, were added to the concretes containing CSA cement. A CEM II A-LL 42.5 R (according to EN197-1) and a commercial CSA cement (i.tech ALI CEM GREEN® by Italcementi) were used. The mixtures proportions are reported in Table 1.

*Table 1. Concrete mixtures design [kg/m$^3$].*

| | CPC | CCSA | CMIX |
|---|---|---|---|
| CEM II-LL 42.5R | 450 | - | 200 |
| CSA ALI CEM | - | 350 | 200 |
| | | | |
| Sand 0.20-0.35 | 258 | 265 | 255 |
| Sand 0.6-1.0 | 197 | 202 | 195 |
| Sand 1.5-2.5 | 262 | 270 | 260 |
| Gravel 3-4 | 142 | 146 | 141 |
| Gravel 6-10 | 335 | 344 | 331 |
| Gravel 10-20 | 584 | 600 | 578 |
| SP (% on binder) | 1.0 | 0.3 | 0.5 |
| Retarder (% on binder) | - | 0.4 | 0.5 |
| Accelerator (% on binder) | - | 0.1 | 0.2 |
| Water | 157.5 | 175 | 180 |
| w/c | 0.35 | 0.50 | 0.45 |

## 2.2. Mixing procedure

Before mixing, all the aggregates were dried at 50% RH. The additional amount of water required to obtain saturated surface dry (SSD) conditions was taken into account in the mix design; an absorption of around 1% by mass in SSD condition was considered for all aggregates. An Eirich R08W high-shear mixer was used. Firstly, all the dry aggregates were placed into the mixer with 1/3 of the total water, followed by mixing for 10 s and a 2 min period of rest to complete the absorption. Afterwards, cement was added and the mixing procedure started, adding gradually the rest of the water and letting it homogenize for 1 min. The admixtures were added thereafter, starting with the superplasticizer followed by the two powders, mixing for 1 min after each addition; the initial consistency was controlled after one more final minute mixing: if it resulted homogeneous, the mixing operation was concluded; otherwise, 1 min more was added to the final step. The total time required by the whole mixing operation was about 5-6 min.

## 2.3. Fresh state properties

Some investigations on the fresh state were performed as quality control measure for each mixture. The Abrams cone was used to measure the workability after mixing (around 7-8 minutes after water

addition) by measuring the slump according to the EN 12350-2 standard. The air content and the density were measured following the EN 12350-6 and EN 12350-7 standards, respectively.

### 2.4. Compressive strength

The measurements of compressive strength were performed at 1, 7 and 28 days following the EN 12390-3 standard on duplicate cubic samples (edge 150 mm) for each age of testing. The samples were produced by filling the plastic molds in two layers and vibrating for 10 s after each pouring. Once the upper surfaces were rectified, the samples in the molds were stored in a climatic room at 20±0.5°C and RH > 95% covered with plastic sheets. The samples were demolded at 24 h and stored in the same climatic room until testing. Before testing, the cubes were polished on the two loading surfaces.

### 2.5. Shrinkage and creep

The volume changes with and without load (creep and shrinkage) were measured both under autogenous and drying conditions following the Swiss standard SIA 262/1:2013 F until 364 days. In particular for creep, CMIX was monitored up to 1 year, while the measurements on the other mixtures were stopped after 182 days because of their substantially stable behaviour, especially when compared to CMIX. It was also decided to deviate from SIA 262/1:2013 F in terms of environmental RH, which was 57% instead of 70% for both shrinkage and creep samples and loading steps applied at different ages. These changes were adopted to observe a higher deformation response (at lower RH) and upgrade the applied stress following the strength evolution.

The specimens were 120×120×360 $mm^3$ prisms cast in stainless steel molds, covered with plastic sheets and stored in the first day after casting in a climatic room at 20±0.5°C and RH > 95%. The samples were demolded after 24 h, when the test started. Two samples were prepared for each test and condition. For every sample, two measuring pins were glued at a distance of 250±1 mm on two opposite sides of the sample, avoiding the cast surface. In this way, two length measurements on each of two samples could be performed. Considering the drying condition, all the surfaces of the sample were exposed to a 20±0.5°C and 57±3% RH environment, while sealed conditions were assured by covering completely the samples with adhesive aluminum tape just after demolding in order to avoid moisture loss. The shrinkage samples were stored horizontally on two thin blade supports, to allow drying from all their surfaces. The duplicate creep samples were placed in hydraulic creep stations vertically one over the other with a metallic plate in between. In this way, the same load could be applied on the duplicate samples. Three sequential loading steps at 1, 7 and 28 days were applied to the samples in order to investigate the initial creep evolution, which is particularly important for the rapid-hardening behavior of CSA cement, and the evolution of creep at increasing load. The first load

step took place after 1 day, the second after 7 days and the last after 28 days, such that the total applied stress $\sigma$ corresponded to 1/3 of the compressive strength at the age of loading (see Fig. 3). However, because of the limited load capacity of the creep testing setups, some samples were loaded at 1/4 of the compressive strength only. These levels of stress were chosen aiming at linear creep behaviour [29].

The deformations were measured manually at selected ages with a comparator equipped with a digital deformation transducer (resolution 0.001 mm corresponding to 4 μm/m for the 250 mm measuring base).The shrinkage and creep results were expressed in terms of strain $\varepsilon$ [μm/m]; the creep data were obtained by subtracting from the total strains the strains due to instantaneous deformation (assumed as occurring between immediately before loading and about 5 min after loading) and subtracting the shrinkage strain measured on the companion shrinkage samples.

All data shown in the graphs in the results section represents the average of two samples and is plotted with its standard deviation.

## 3. RESULTS

### 3.1. Fresh state

A summary of the results on fresh concrete is reported in Table 2. Considering CPC and CMIX, the density was slightly lower than expected at the mix design stage, when a value of 1.5% of entrained air was considered; the corresponding differences were also found for the air content. In terms of slump, high initial workability for the CSA based mixtures was found, with no aggregate segregation.

*Table 2. Details of the fresh state tests*

| | | CPC | CCSA | CMIX |
|---|---|---|---|---|
| Initial slump* [mm] | | 180 | 250 | 225 |
| Density [kg/m$^3$] | measured | 2368 | 2355 | 2309 |
| | mix design | 2392 | 2352 | 2346 |
| Air content [%] | | 2.5 | 1.3 | 3.2 |

*Measured at the end of casting operations, 7-8 min after water addition

### 3.2. Compressive strength

The compressive strength evolution was monitored until 28 days; the results are reported in Figure 1. Compared to the previous study on the same mixture compositions [23], these mixtures reached lower compressive strength at 28 days due to the higher amount of entrained air, probably connected to the different mixer used in this campaign.

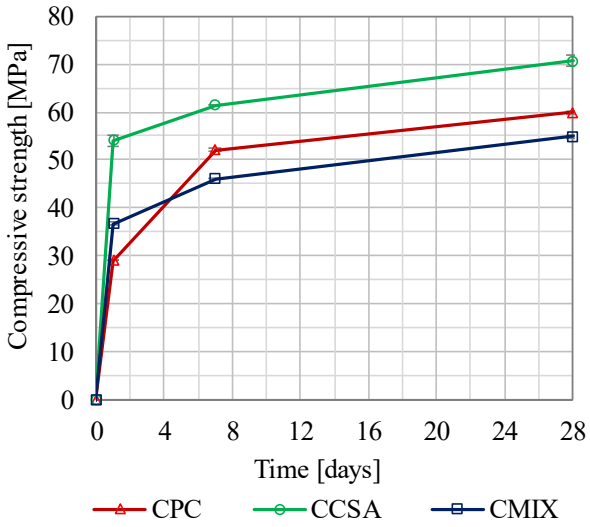


*Figure 1. Compressive strength results. Average and standard deviation of 2 samples.*

### 3.3. Shrinkage

Results of shrinkage under both autogenous and drying conditions are reported in Figure 2. The dotted lines indicate the sealed condition, while continuous lines indicate samples exposed to the environment of the climatic room (20°C and 57% RH). In drying conditions, CPC showed the fastest evolution and the highest final value of shrinkage. At the same time, in autogenous conditions the final shrinkage at 1 year was similar for all the mixtures (-212, -204, -228 µm/m for CPC, CCSA and CMIX, respectively). While CPC and CCSA followed the same trend, CMIX showed a particular evolution in time: initial shrinkage was observed up to 7 days, followed by expansion until 28 days and a more stable period up to 35 days. From that point on, CMIX started to shrink again: first rapidly until 56 days, then at a slower steady rate. During this second shrinking period, the curve for autogenous conditions crosses the shrinkage curve in drying conditions (the difference remains however small, about 50 µm/m).

The overall result is lower total shrinkage for CCSA and CMIX compared to CPC, especially in drying conditions.

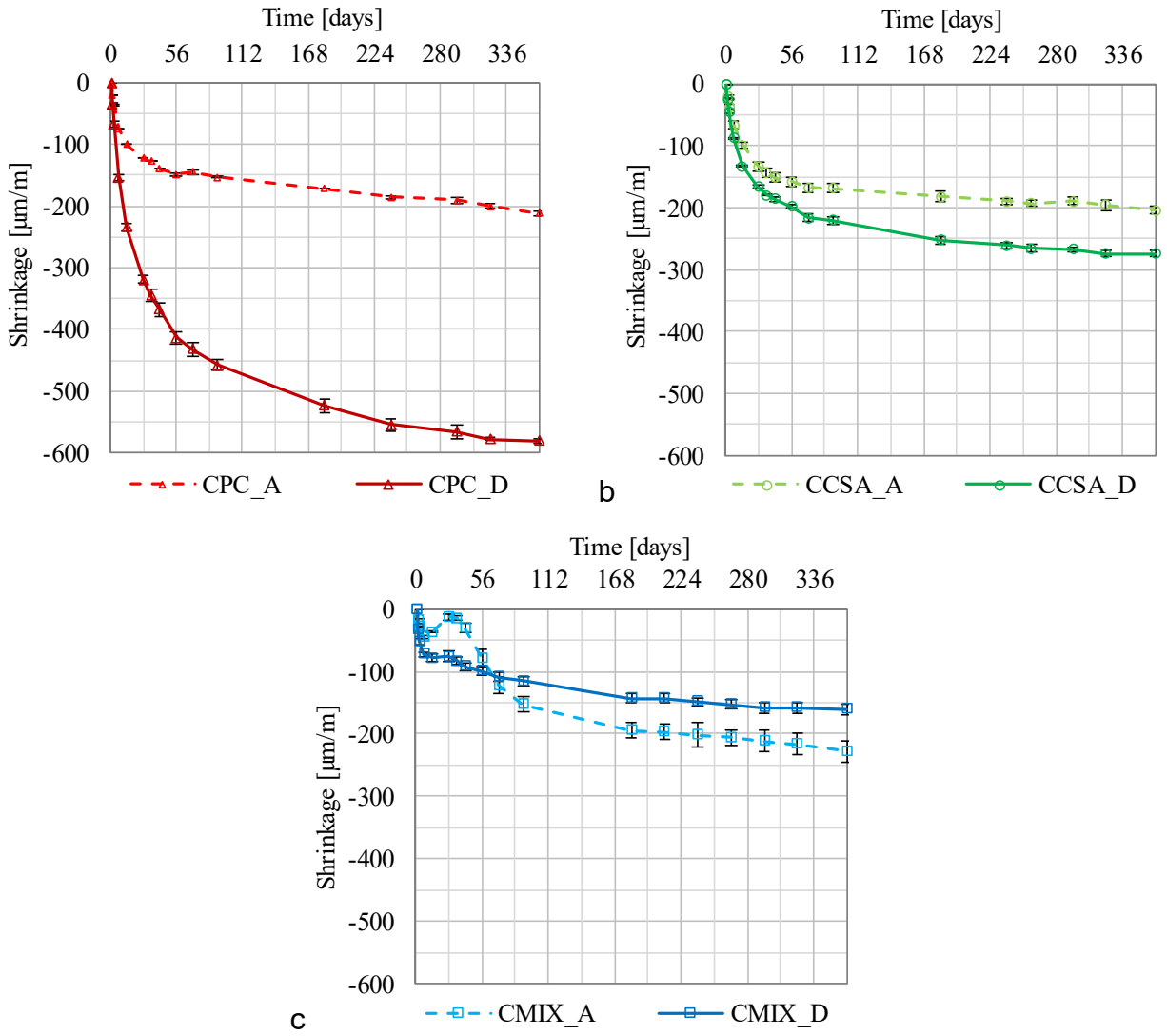


*Figure 2. Autogenous (_A) and drying (_D) shrinkage results. Average and standard deviation of 2 samples.*

### 3.4. Creep

Figure 3 shows the creep evolution for the three mixtures. The results under autogenous and drying conditions are reported, corresponding to basic and drying creep, respectively. When one considers different values of the applied stress (note in particular considerably lower applied stress at 1 d for the CPC than for the other concretes), it becomes evident that the specific creep (i.e. creep per applied stress) was considerably higher for the CPC compared to CCSA and CMIX, in particular in drying conditions. Furthermore, the difference between the drying and basic creep was the highest for the CPC system. An interesting trend could be observed for the blended system, CMIX, where the basic creep became larger than the drying creep after about 42 d; similar behaviour of larger deformations in sealed than in drying conditions could be observed for shrinkage results in Fig. 2c.

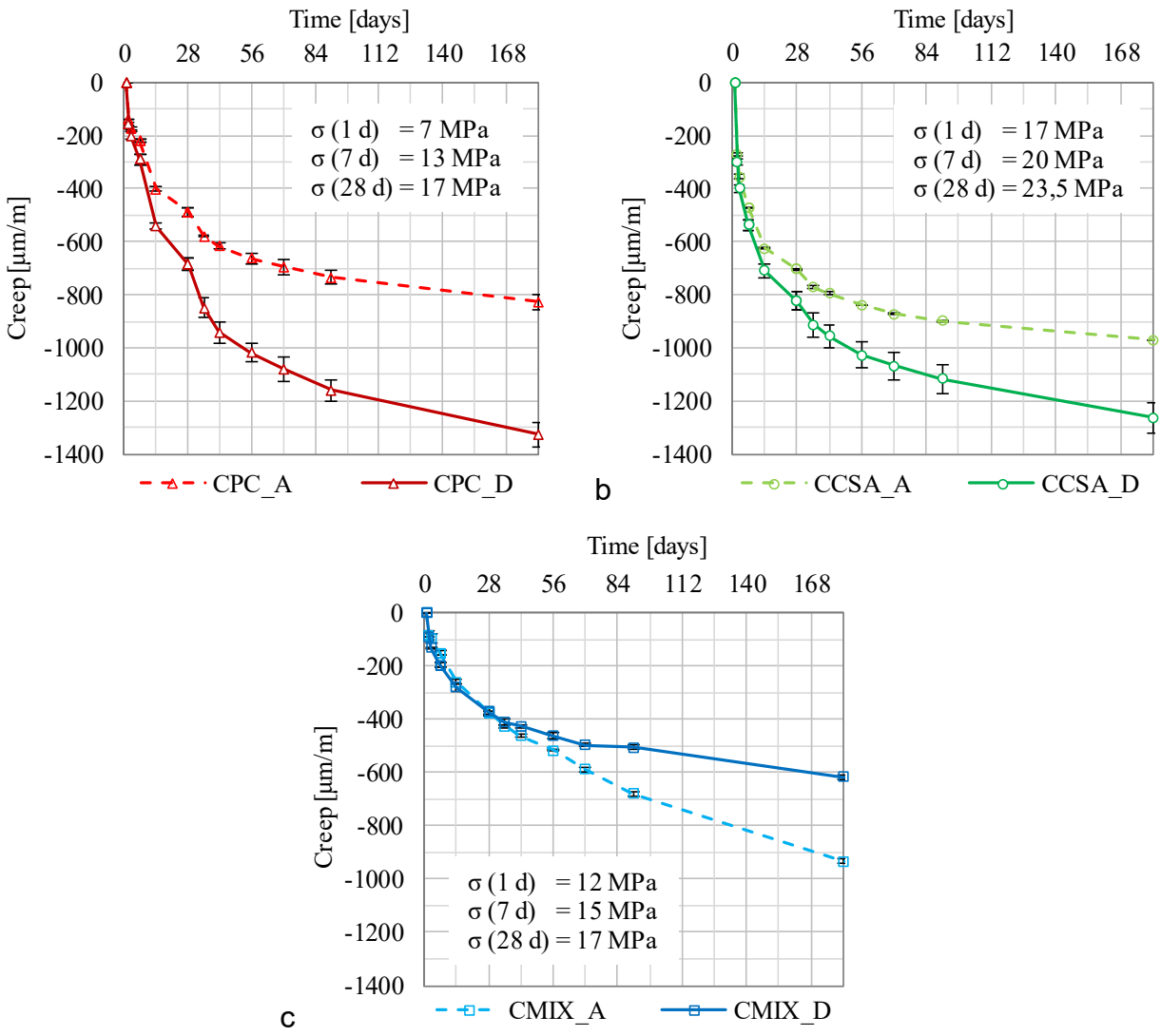


*Figure 3. Basic (_A) and drying (_D) creep results. Stresses applied at 1, 3 and 28 d are indicated.*

## 4. DISCUSSION

### 4.1. Differences between autogenous and drying conditions

The measurements of shrinkage and creep both in sealed conditions (autogenous shrinkage and basic creep) and in drying conditions (drying shrinkage and drying creep) may be considered representative of the boundaries of the concrete behaviour in the field (when one disregards the inevitable temperature changes). Sealed conditions are characteristic of the concrete before demolding, when no moisture exchange between the material and the outer environment takes place, while drying conditions occur after demolding. Considering then concrete elements of large dimensions, the core can be considered to hydrate in sealed conditions, while the surface undergoes drying.

Before examining the volume changes of the concrete mixtures, it must be pointed out that the microstructure and the pore structure of the matrix depend strongly on the binder used. The PC-based systems contain mainly calcium-silicate hydrate (C-S-H), whose creep and shrinkage and their strong dependence on RH are well known [30]. On the other hand, the main hydrated phase of CSA is

ettringite, with morphology and porosity radically different from C-S-H. Ettringite is expected to be dimensionally quite stable and less sensitive to changes in RH [31,32]. Hence, different shrinkage and creep behaviours are expected from concrete made with PC and CSA binders.

The PC mixture showed the highest difference between autogenous and drying shrinkage. This is generally observed in concrete based on Portland cement, with the relative importance of autogenous shrinkage compared to drying shrinkage growing with the decrease of w/c [19].

On the contrary, in CCSA the self-desiccation shrinkage is very close to the total shrinkage measured at 57% RH. This may be due to the combination of rapid self-desiccation and a very tight pore structure that limits further water loss in drying conditions [33]. While the autogenous shrinkage of CPC and CCSA are similar, the total shrinkage in drying conditions is much lower in CCSA.

A radically different picture is given by CMIX: in sealed conditions, after an expansion phase [34,35] that ends at about 28 days, autogenous shrinkage followed at high rate and surpassed the total shrinkage in drying conditions after 70 days. The observed trend was different with respect to PC, since the total shrinkage in drying conditions is usually found to be higher than autogenous shrinkage, when the environmental RH is lower than the internal RH in sealed conditions. According to the results obtained on mortars with the same binders as used here for concrete, the internal RH in autogenous conditions after 56 days is around 86% and appears to be stable [36]. This value is not expected to drop much further, since Portland cement hydration will not proceed when the RH is below about 70-80% [37–40] and the hydration of the CSA should be finished by that time. Hence, the internal RH in autogenous conditions should be much higher than the equilibrium RH of the drying specimens (57%).

Both drying and autogenous shrinkage can be described by the Biot-Bishop equation [41], a classical poromechanics approach that approximates the linear elastic deformation of an unsaturated porous body under the action of pore pressure:

$$\varepsilon_v = -S_w \cdot p \cdot (1/K_b - 1/K_s) \quad (1)$$

where $S_w$ (-) is the volumetric saturation degree, $p$ (Pa) is the pore pressure, $K_b$ (Pa) is the drained bulk modulus of the porous body and $K_s$ (Pa) is the bulk modulus of its solid skeleton. The pore pressure can be calculated with the Kelvin-Laplace equation (neglecting the effect of the ions in the pore solution on the internal RH [42–44]):

$$p = \rho \cdot R \cdot T \cdot \ln(RH)/M \quad (2)$$

where $\rho$ (kg/m$^3$) is the density of the pore fluid, assumed as 1000 kg/m$^3$, $R$ is the universal gas constant equal to 8.314 [J/(mol K)], $T$ (K) is the test temperature (293.15K) and $M$ (kg/mol) is the molar mass of the pore fluid, assumed equal to that of water, 0.01802 kg/mol.

If one considers the different pore pressures acting on the CMIX specimens at equilibrium, the pore pressure in the drying specimens (57% RH) should be always higher than in the specimens in sealed conditions (>80% RH) and hence higher shrinkage should be expected for the drying specimens. However, according to the Biot-Bishop equation (Eq. 1), it would be possible to reach higher autogenous deformation than drying shrinkage if the degree of saturation is substantially different between the two conditions (i.e. higher in the autogenous conditions). It is worth to underline that not only the classical Biot-Bishop approach, but also other poromechanics approaches, e.g. [45–47] would predict higher shrinkage for higher water contents (here expressed with saturation degree) when the pore pressure is the same. The degree of saturation is used to describe the effect of the pore fluid pressure acting only on part of the solid skeleton in unsaturated conditions.

In CMIX at initial stages of hydration, a coarse pore structure permits a substantial moisture loss at short drying times [36,48]. In such case, the degree of saturation would drop in drying conditions and, even if the pore fluid pressure is high, the average pore pressure acting on the skeleton could be smaller than in autogenous conditions.

In addition, the blended system CMIX shows two distinct hydration phases [36]. For the mortars systems with exactly the same binder as in CMIX, it was concluded that the calcium sulfoaluminate cement reacts immediately after the first addition of water and shows hardly any further reaction after the first week [36]. On the other hand, Portland cement hydration is slower in these systems and does not start until about 3 to 4 weeks after water addition [36]. In autogenous conditions, the internal RH is high enough (about 94% RH was measured in the mortars from 3 to 28 days [36]), to allow hydration of the Portland cement. Cement hydration then induces self-desiccation (the RH decreased to 86% at 56 days [36]) and autogenous shrinkage. The onset of hydration of the Portland cement occurring within the matrix of already hydrated calcium sulfoaluminate cement could also be responsible for the expansion observed between 7 and 28 days (Figure 2c), likely due to crystallization pressure of crystalline hydration products of the Portland cement [49] and possibly due to hygral swelling (note that a slight increase of RH between 3 and 14 days was observed on the corresponding mortar in [36]). On the other hand, in the concrete specimens exposed to drying at early ages, a large amount of moisture is lost, with the consequence that the further reaction of the Portland cement might not occur or occur only to a smaller extent. This would result in no further pore refinement and lower degree of saturation compared to autogenous conditions. While these phenomena would be able to qualitatively explain the observed higher autogenous shrinkage of CMIX compared with its total shrinkage in drying conditions, further research is needed to explain these differences quantitatively. In particular, the different phase composition of the binder in the concrete mixtures (CPC main hydrate C-S-H; CCSA, ettringite and aluminum hydroxide; CMIX ettringite plus

C-S-H) and the very different kinetics of hydration of the clinkers may help explaining their shrinkage behavior (see also [36]).

The basic creep of CPC is slightly lower compared to CCSA. However, considering the higher strength of CCSA, especially at early ages, and hence the higher applied load, the specific creep of CPC is higher. This can be explained as an effect of: 1) higher mechanical properties (see Fig. 1), and hence possibly also lower creep compliance of the CCSA, and/or 2) by the fact that most of the hydration of the calcium sulfoaluminate cement is over by 1 day of age, when the specimens are exposed to drying, while the Portland cement in CPC would keep reacting for much longer time. The latter explanation is according to a recent model for creep [50], where cement hydration and the resulting dissolution of elastic clinker while the system is subject to external load has been suggested as an important contribution to early-age creep (see also [51]). As regards mechanism 1 (lower specific creep of the CCSA system), it should be also noted that is very likely that the inherent creep properties of the hydration products in the CCSA system are considerably different (here, lower) than in the CPC system. In a microindentation study performed on compacts of hydration products [52], C-S-H had greater creep rate than any other tested hydration product, including ettringite. However, also ettringite exhibited microindentation creep.

Regarding the basic creep of the blended system, CMIX is in between the results of the other two systems (considering the applied stresses); the kinetics are clearly different, with gradual increase in basic creep after 2-3 months, while a more pronounced reduction in creep rate could be observed for the other systems. Moreover, the fact that the basic creep of CMIX is higher than its drying creep (the two curves cross at about 70 days), is in line with the free shrinkage results discussed above. This behaviour could be again attributed to long-term, slow hydration of the Portland cement that goes on under external load [50] in the sealed system, while it stops due to insufficient water in the drying system. In the drying system, a moisture gradient and a gradient of degree of hydration (lower degree of hydration close to the surface compared to the centre of the specimen) are expected. The drying front would penetrate more deeply into the sample in the case of slow hydration, i.e. drying would be more important for CMIX compared to CCSA.

As regards drying creep, a much higher impact of moisture loss on the creep response could be observed for the CPC system compared to the systems containing CSA binder. Again, this difference may be due to the different hydration products in these systems and hence inherently different creep (both basic and drying) properties.

The volume stability, both in terms of shrinkage and creep, is a major concern when dealing with durability of concrete structures. In general, limiting creep is paramount to avoid large deformations of loaded structures, which may lead to failure in extreme cases [53] or to prestress losses [54]. In its turn, shrinkage needs to be limited to avoid that the build-up of restraint stresses causes early-age

cracks [55–57], which may reduce the service life of concrete structures. In CPC, the large difference between autogenous and drying shrinkage may induce cracking due to self-restraint in elements with large cross section, since the inner part of the element (in autogenous conditions) shrinks considerably less than the outer layer (in drying conditions). In these terms, both CSA-based systems examined in this study (CCSA and CMIX) would be advantageous, because of their lower shrinkage under drying conditions and because of the smaller difference between autogenous and drying shrinkage. For this latter characteristic, these blended systems are similar to HPC and even more to UHPC [58], in which the contribution to the total shrinkage originating from self-desiccation progressively increases with the decrease of w/c.

However, while the long-term shrinkage of CCSA and CMIX does not seem to be of concern, particular attention is required during the very early age. As calcium sulfoaluminate cement is characterized by rapid hydration, self-desiccation and autogenous shrinkage develop at an extremely fast rate already in the first day (evident in a parallel study on mortars [36]), before the start of the length change measurements in this study. Such rapid autogenous shrinkage, which is uniform on the whole cross section of the concrete element, could be counteracted or at least delayed by means of internal curing [59,60]. If self-desiccation and the accompanying shrinkage occur later at a lower rate, there may be sufficient time for stress relaxation (the other manifestation of the viscoelastic properties besides creep) to reduce the stresses so that macroscopic cracking is avoided [61].

A final consideration should be made on the creep behaviour of CCSA and CMIX (Figure 3b and c). While for a given applied stress their lower creep compared to CPC would be beneficial, e.g. in limiting the long-term deformation of reinforced concrete structures or prestress losses in prestressed structures, the low creep at early ages may also limit stress relaxation and increase the probability of cracking due to restraint stresses [61,62]. This aspect would require to be investigated in detail in further research. Another important aspect is the characteristic basic creep of CMIX (Figure 3c), which increased steadily even after 6 months of loading.

Such a behaviour was even more evident on the measurements made on mortar specimens with the same binders [36]: this could be reasonably linked to the slow reaction of the Portland cement in CMIX when enough water is available in sealed conditions, manifesting as dissolution creep [50] when subjected to mechanical load. This aspect should be investigated in depth before HPC based on blends of PC and CSA cements is used in practical applications as structural concrete.

### 4.2. Comparison with predictions according to Model Code 2010 and ACI 209.R-92

The different regional or national codes contain calculation approaches for both shrinkage and creep of concrete; notable examples are ACI 209.R-92 (1992) [26] and CEB-FIP Model Code 2010 (2010) [25]. Usually, these formulas are based on the knowledge of the 28-days compressive strength of the

concrete (or more generally, on the concrete strength class), which is the most widely measured property. In addition, a number of other parameters related to the environmental conditions and the geometry of the concrete member (in particular, to its surface-to-volume ratio) play a role in these formulas.

These empirical formulas are based on curve fitting of a large amount of experimental data collected through several decades [63] and almost exclusively regarding normal strength concrete based on Portland cement. Some of these models were recently upgraded to better cover HPC (characterized by rapid hydration and high autogenous shrinkage) and loading at early ages, which is made possible by the very fast strength development [63].

In addition, even for relatively small changes between pure Portland cement and blended cements with different types and amounts of supplementary cementitious materials, rather different creep and shrinkage values were measured [22,62]. Given the above, when pure CSA cements or blends of CSA and PC are considered, both their drying behaviour and the deformation as a consequence of self-desiccation and external loads might be radically different from that of concrete of the same strength class based on Portland cement, as discussed in the previous section.

In this section, a comparison of the measured creep and shrinkage results (both in sealed and in drying conditions) with the empirical formulas according to Model Code 2010 [25] and ACI 209.R-92 [26] is presented.

Considering the creep deformation, the comparison was done in terms of strain (i.e., the total deformation under load after deduction of elastic deformation and shrinkage). In the empirical models, the creep strain was obtained from the creep coefficient prediction, multiplying it by the ratio between the applied stress (which generated the deformation) and the Young's modulus of elasticity at 28 days, calculated from the mean cylindrical compressive strength. The final creep strain is the result of the superposition of three creep coefficient values, as reported in eq. (3), one for each loading step. The first, for age of loading 1 d, was considered throughout the whole investigated period and related to the entire stress applied at 1 d; the second, with age of loading 7 d, was calculated with the incremental stress applied at 7 d (i.e. stress at 7 d minus stress at 1 d); the last, for age of loading 28 d, was calculated with the incremental stress applied at 28 d.

$$\varepsilon_{cc}(56d) = \frac{\sigma_c(1d)}{E_{28d}} \cdot \varphi(56d, 1d) + \frac{\sigma_c(7d)-\sigma_c(1d)}{E_{28d}} \cdot \varphi(56d, 7d) + \frac{\sigma_c(28)-\sigma_c(7d)}{E_{28d}} \cdot \varphi(56d, 28d) \quad (3)$$

where

$\varepsilon_{cc}(t)$ creep strain at time $t$;

$\sigma_c(t_0)$ applied constant stress at time $t_0$;

$E_{ci}$ dynamic modulus of elasticity at age 28 days;

$\varphi(t, t_0)$ creep coefficient at time $t$, for load applied at time $t_0$;

The Model Code 2010 describes both creep and shrinkage as the sum of two parts: one due to autogenous conditions and the other due to drying. These two terms were added when calculating the drying shrinkage and the drying creep. Conversely, ACI 209.R-92 does not distinguish between autogenous and drying conditions; it considers just one formulation describing the total deformation for a structure exposed to drying. As a consequence, ACI 209.R-92 was used only for predicting the total shrinkage in drying conditions and the drying creep. More details about the Model Code 2010 and ACI 209.R-92 formulations are reported in Appendix A.

Due to their generality and inherent simplifications, it can be expected that the predictive power of these empirical approaches may be limited. In addition, since these formulations are based on the superposition effect, interactions between drying and external loads (i.e. the Pickett effect [64]) cannot be taken into account.

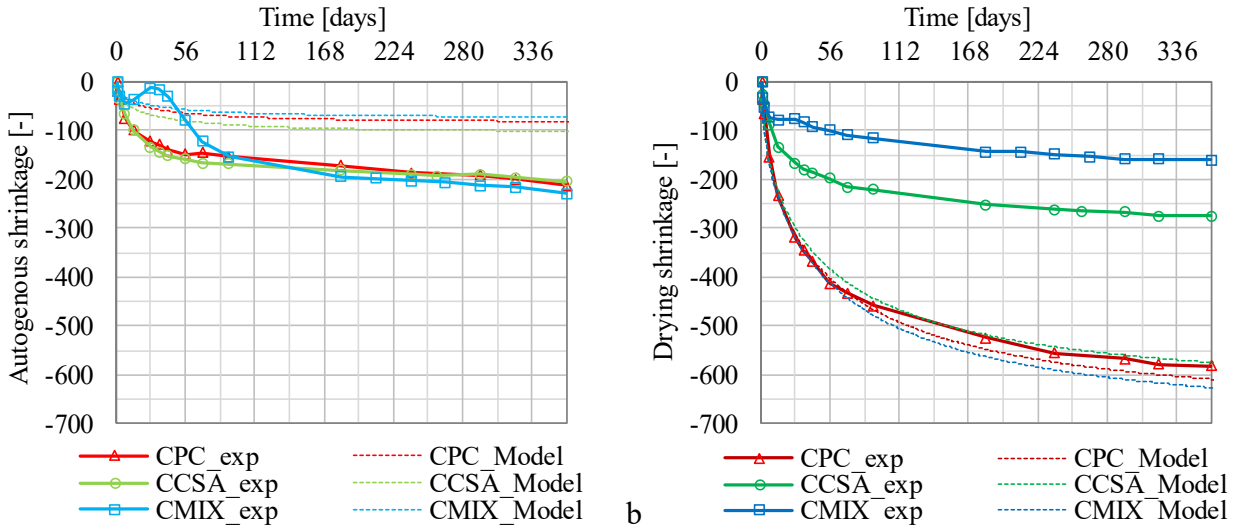


*Figure 4. Comparison between experimental and modelled shrinkage evolution in both autogenous (a) and drying (b) conditions by Model Code 2010.*

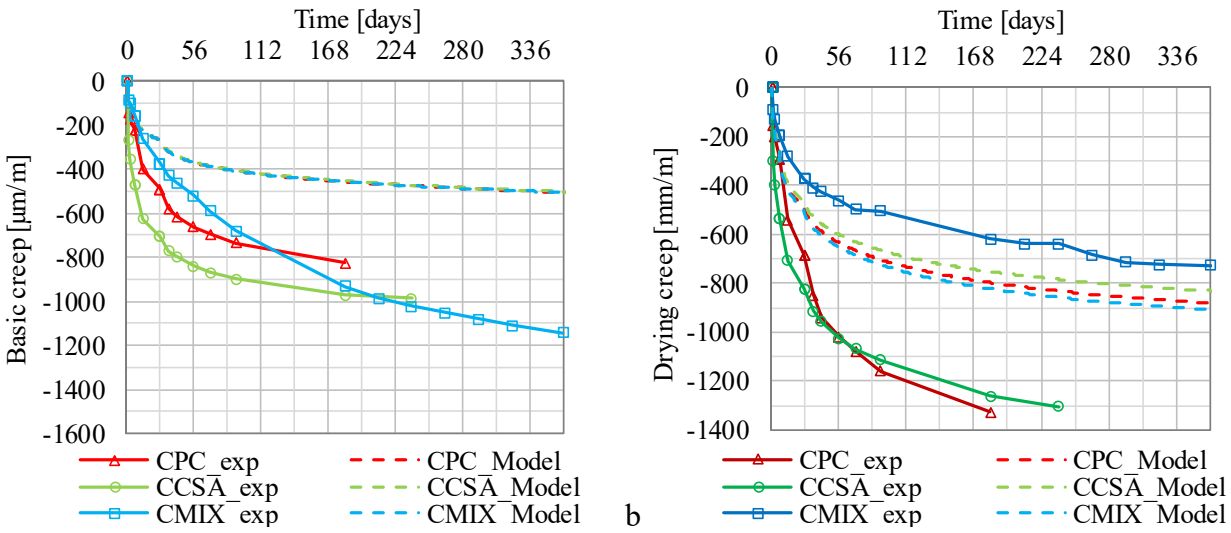


*Figure 5. Comparison between experimental and modelled creep evolution in both autogenous (a) and drying (b) conditions by Model code 2010*

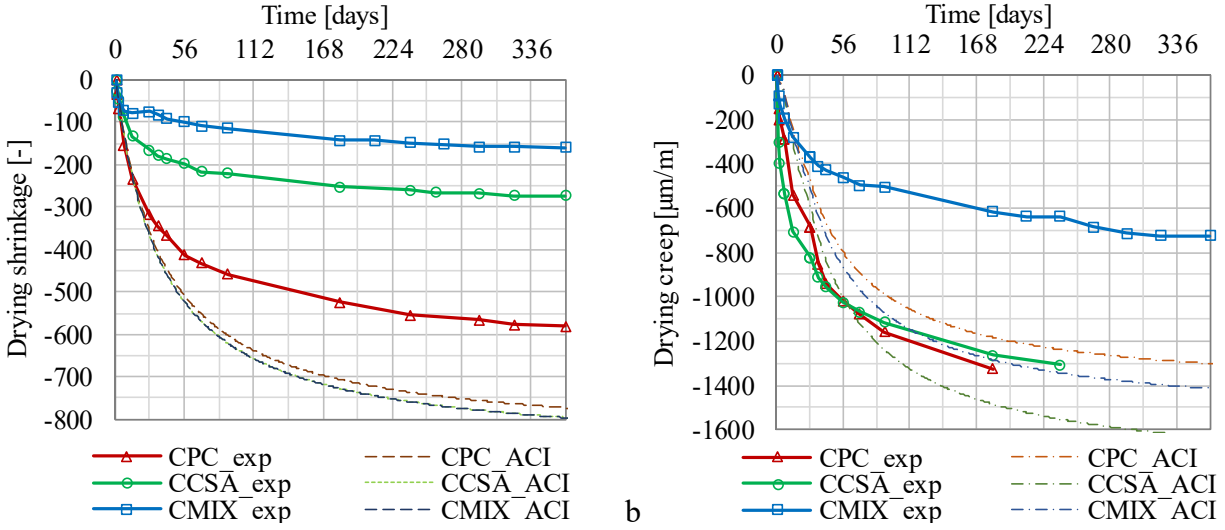


*Figure 6. Comparison between experimental and modelled shrinkage (a) and creep (b) evolution in drying conditions by ACI 209.R-92.*

Figure 4-6 show the comparison between the predictions with Model Code 2010 and ACI 209.R-92 both for creep and shrinkage evolution and the corresponding experiments.

Regarding the shrinkage, Model Code 2010 (Figure 4) predicts very well the total shrinkage under drying conditions of the PC system, while the autogenous shrinkage of sealed specimens is underestimated (by more than 50%). Considering that the Model Code 2010 calculates the total shrinkage under drying conditions as the sum of an autogenous shrinkage contribution and a drying shrinkage contribution (see Appendix A), these findings lead to the conclusion that the drying shrinkage contribution to the total shrinkage in drying conditions tends to be overestimated. In the cases of CCSA and CMIX, Model Code 2010 underestimates the shrinkage in sealed conditions

similarly as for CPC, while it overestimates considerably the shrinkage in drying conditions. While for CCSA the predicted shrinkage is more than twice the experimental value, the overestimation for CMIX is more than fourfold. On the other hand, ACI 209.R-92 (Figure 6a) overestimates the ultimate shrinkage in drying conditions by about 15%; while the shape of the curves is similar; after 28 days the predicted deformation increases faster than the experimental.

Compared to ACI 209.R-92, Model Code 2010 predicts more accurately the short term deformation after the load increments. However, for both autogenous and drying conditions, the long-term deformation is underestimated for the PC system. On the contrary, the ACI model is less accurate in the short term after loading but predicts ultimate values close to those obtained experimentally for the PC system.

The predictions of basic creep according to Model Code 2010 (Figure 5a) underestimate considerably the experimental results for all three concrete mixtures (the predictions are about half of the experimental values). The case of drying creep predictions with Model Code 2010 (Figure 5b) is similar for the CPC and CCSA, while for CMIX the predictions are about 35% higher. On the contrary, ACI 209.R-92 (only for drying creep) seems to be more precise when predicting drying creep of CCSA and CPC (10% and 20% difference, respectively, see Figure 6b), while it overestimates considerably the drying creep of CMIX.

When only CPC is considered, it appears that both models give reasonably good predictions in terms of drying shrinkage; furthermore ACI 209.R-92 seems reliable for drying creep as well. The autogenous shrinkage and basic creep models in Model Code 2010 appear to underestimate the deformations considerably.

Given the above, while the accuracy of these models cannot obviously be judged based only on few experimental results, the differences in sealed conditions are rather large and may be worth a deeper investigation at these models in further research.

For the systems based on calcium sulfoaluminate cement (CCSA and CMIX), it can be concluded that the experimental results are considerably different from the predictions of both models. Nevertheless, under drying conditions, the shape of the experimental and predicted curves is similar and the order of magnitude is the same. Thus, it is expected that special factors can be defined for the equations used in both Model Code 2010 and ACI 209.R-92 (see Appendix A) in order to take into account the initial rapid and intense self-desiccation and autogenous shrinkage of CCSA and the smaller overall deformation of CMIX that were observed under all conditions. Finally, for CMIX made with blended cement, the autogenous deformation showed a succession of shrinkage and expansion phases that would require entirely different models. Similarly, the fact that the basic creep of CMIX was larger than the drying creep would require an *ad-hoc* description different from the current approach in Model Code 2010.

485 If CSA cement and blends with Portland cement are to be included in practical models as Model Code
486 2010 and ACI 209.R-92, a large basis of experimental data covering multiple concrete mixtures,
487 geometries, exposure and loading conditions will be required.
488 In the meantime, based on projects like the one described in this paper, a database with measurements
489 of mechanical properties, deformation behaviour and durability indicators of structural concrete based
490 on blends of CSA and Portland cement will be established. This will help concrete producers,
491 engineers and contractors in the choice of appropriate mixture compositions for the different practical
492 applications until mature engineering models for concrete with these novel binders become available.
493
494 **5. CONCLUSIONS**
495 In this research, the shrinkage and creep evolution in both autogenous and drying conditions of HPC
496 based on CSA cement and blends of CSA with Portland cement were studied.
497 Three concrete mixtures based on different cement systems were investigated: a Portland-limestone
498 cement (CEM II-LL 42.5R), a commercial CSA and a blend of the two previous cements at ratio of
499 50/50 by mass.
500 Both the creep and the shrinkage of CSA-based systems were lower than for the PC system. The
501 concrete with pure CSA cement showed rapid and significant self-desiccation and autogenous
502 shrinkage, while the additional shrinkage in drying conditions was limited. CSA-based mixtures
503 showed also lower differences between basic and drying creep. On the contrary, CPC reacts slowly
504 and the differences between autogenous shrinkage and drying shrinkage, and between basic and
505 drying creep are significant. The blended system CMIX showed the lowest deformation in both
506 shrinkage and creep when exposed to drying, with limited differences between drying and sealed
507 conditions. Interestingly, both shrinkage and creep in sealed conditions were slightly higher than in
508 drying conditions, which may be explained by continued hydration, pore refinement and higher
509 degree of saturation of the sealed systems.
510 The measured creep and shrinkage of these concrete mixtures were then compared to the empirical
511 models according to Model Code 2010 and ACI 209.R-92, which were developed based on Portland
512 cement. While the predictions of the deformation of the PC concrete under drying conditions were
513 satisfactory, Model Code 2010 underestimated the deformation in sealed conditions (ACI 209.R-92
514 does not cover this case). For CCSA and CMIX, different empirical factors should be defined in the
515 models so as to take into account the initial strong self-desiccation of CCSA and the global lower
516 shrinkage of CMIX. On the other hand, previous studies found that current empirical models are
517 effective in predicting compressive strength and modulus of elasticity of these mixtures. While the
518 definition of special models for the deformation behaviour (shrinkage and creep) of CSA cements in
519 these codes would need a substantial basis of experimental work, the results presented in this paper,

520 together with other ongoing campaigns, can be an initial guidance for engineers and contractors that
521 are working with CSA cement.
522
523 **6. REFERENCES**

524 [1] M.C.G. Juenger, F. Winnefeld, J.L. Provis, J.H. Ideker, Advances in alternative cementitious
525 binders, Cem. Concr. Res. 41 (2011) 1232–1243. doi:10.1016/j.cemconres.2010.11.012.
526 [2] F.P. Glasser, L. Zhang, High-performance cement matrices based on calcium sulfoaluminate-
527 belite compositions, Cem. Concr. Res. 31 (2001) 1881–1886. doi:10.1016/S0008-
528 8846(01)00649-4.
529 [3] F. Winnefeld, B. Lothenbach, Hydration of calcium sulfoaluminate cements - Experimental
530 findings and thermodynamic modelling, Cem. Concr. Res. 40 (2010) 1239–1247.
531 doi:10.1016/j.cemconres.2009.08.014.
532 [4] J. Péra, J. Ambroise, E. Holard, G. Beauvent, Influence of the type of calcium sulfate on the
533 properties of calcium sulfoaluminate cement, in: 11th Int. Congr. Chem. Cem., 2003: pp.
534 1129–1135.
535 [5] L. Pelletier, F. Winnefeld, B. Lothenbach, The ternary system Portland cement-calcium
536 sulphoaluminate clinker-anhydrite: Hydration mechanism and mortar properties, Cem. Concr.
537 Compos. 32 (2010) 497–507. doi:10.1016/j.cemconcomp.2010.03.010.
538 [6] W. Lan, F.P. Glasser, Hydration of calcium sulphoaluminate cements, Adv. Cem. Res. 8
539 (1996) 127–134.
540 [7] L. Zhang, F.P. Glasser, Hydration of calcium sulfoaluminate cement at less than 24 h, Adv.
541 Cem. Res. 14 (2002) 141–155. doi:10.1680/adcr.2002.14.4.141.
542 [8] D. Sirtoli, S. Tortelli, P. Riva, M. Marchi, R. Cucitore, M.N. Rose, Mechanical and durability
543 performances of sulpho-based rapid hardening concrete, ACI Spec. Publ. 305 (2015) 1–8.
544 [9] L. Zhang, M. Su, Y. Wang, Development of the use of sulfo- and ferroaluminate cements in
545 China, Adv. Cem. Res. 11 (1999) 15–21. doi:10.1680/adcr.1999.11.1.15.
546 [10] M.S. Meddah, M. Suzuki, R. Sato, Influence of a combination of expansive and shrinkage-
547 reducing admixture on autogenous deformation and self-stress of silica fume high-performance
548 concrete, Constr. Build. Mater. 25 (2011) 239–250. doi:10.1016/j.conbuildmat.2010.06.033.
549 [11] S. Slatnick, K.A. Riding, K.J. Folliard, M.C.G. Juenger, A.K. Schindler, Evaluation of
550 autogenous deformation of concrete at early ages, ACI Mater. J. 108 (2011) 21–28.
551 doi:10.14359/51664212.
552 [12] T. Noguchi, P. Sun-Gyu, I. Maruyama, Mechanical properties of high-performance concrete
553 with expansive additive and shrinkage reducing admixtures under simulated completely-
554 restrained condition at early age, in: Self-Desiccation Its Importance Concr. Technol. Proc. 4th

555 Int. Semin., 2005.
556 [13] J. Péra, J. Ambroise, New applications of calcium sulfoaluminate cement, Cem. Concr. Res.
557 34 (2004) 671–676. doi:10.1016/j.cemconres.2003.10.019.
558 [14] J. Ambroise, J. Péra, Use of calcium sulfoaluminate cement to improve strength of mortars at
559 low temperature, Concr. Repair, Rehabil. Retroffiting II. (2009) 881–886.
560 [15] L. Pelletier-Chaignat, F. Winnefeld, B. Lothenbach, C.J. Müller, Beneficial use of limestone
561 filler with calcium sulphoaluminate cement, Constr. Build. Mater. 26 (2012) 619–627.
562 doi:10.1016/j.conbuildmat.2011.06.065.
563 [16] I.A. Chen, C.W. Hargis, M.C.G. Juenger, Understanding expansion in calcium sulfoaluminate-
564 belite cements, Cem. Concr. Res. 42 (2012) 51–60. doi:10.1016/j.cemconres.2011.07.010.
565 [17] J. Weiss, P. Lura, F. Rajabipour, G. Sant, Performance of Shrinkage-Reducing Admixtures at
566 Different Humidities and at Early Ages, ACI Mater. J. 105 (2008). doi:10.14359/19977.
567 [18] O. Mejlhede Jensen, P. Freiesleben Hansen, Autogenous deformation and change of the
568 relative humidity in silica fume-modified cement paste, ACI Mater. J. 93 (1996) 539–543.
569 doi:10.14359/9859.
570 [19] P. Lura, O.M. Jensen, K. Van Breugel, Autogenous shrinkage in high-performance cement
571 paste: An evaluation of basic mechanisms, Cem. Concr. Res. 33 (2003) 223–232.
572 doi:10.1016/S0008-8846(02)00890-6.
573 [20] P. Lura, F. Winnefeld, X. Fang, A simple method for determining the total amount of
574 physically and chemically bound water of different cements, J. Therm. Anal. Calorim. (2015)
575 1–8.
576 [21] S.I. Igarashi, A. Bentur, K. Kovler, Autogenous shrinkage and induced restraining stresses in
577 high-strength concretes, Cem. Concr. Res. 30 (2000) 1701–1707. doi:10.1016/S0008-
578 8846(00)00399-9.
579 [22] P. Lura, K. Van Breugel, I. Maruyama, Effect of curing temperature and type of cement on
580 early-age shrinkage of high-performance concrete, Cem. Concr. Res. 31 (2001) 1867–1872.
581 doi:10.1016/S0008-8846(01)00601-9.
582 [23] D. Sirtoli, P. Riva, S. Tortelli, M. Marchi, Mechanical performance of sulpho-based rapid
583 hardening concrete, in: New Boundaries Struct. Concr. Sess. C - New Scenar. Concr., 2016.
584 [24] D. Sirtoli, P. Riva, S. Tortelli, M. Marchi, Mechanical Performance Comparison Between
585 Sulfo-Based and Portland Concretes, Spec. Publ. (2018).
586 [25] J. Walraven, Model Code 2010, final drafts, FIB Bull. 1 & 2 (2012) 105.
587 [26] ACI Committee 209, ACI 209R-92 Prediction of Creep, Shrinkage,and Temperature Effects
588 in Concrete Structures, 2008. doi:10.1201/9780203882955.ch168.
589 [27] L.H.J. Martin, F. Winnefeld, C.J. Müller, B. Lothenbach, Contribution of limestone to the

hydration of calcium sulfoaluminate cement, Cem. Concr. Compos. 62 (2015) 204–211. doi:10.1016/j.cemconcomp.2015.07.005.

[28] T. Matschei, B. Lothenbach, The role of calcium carbonate in cement hydration, Cem. Concr. Res. 37 (2007) 551–558.

[29] Z.P. Bazant, Mathematical modelling of creep and shrinkage of concrete, Matheatical Model. Creep Shrinkage Concr. (1988) 99–215.

[30] H.M. Jennings, Colloid model of C-S-H and implications to the problem of creep and shrinkage, Mater. Struct. (2003). doi:10.1617/14137.

[31] L.G. Baquerizo, T. Matschei, K.L. Scrivener, Impact of water activity on the stability of ettringite, Cem. Concr. Res. (2016). doi:10.1016/j.cemconres.2015.07.008.

[32] J. Kaufmann, F. Winnefeld, B. Lothenbach, Stability of ettringite in CSA cement at elevated temperatures, Adv. Cem. Res. (2016). doi:10.1680/jadcr.15.00029.

[33] J. Bizzozero, C. Gosselin, K.L. Scrivener, Expansion mechanisms in calcium aluminate and sulfoaluminate systems with calcium sulfate, Cem. Concr. Res. 56 (2014) 190–202. doi:10.1016/j.cemconres.2013.11.011.

[34] P. Chaunsali, P. Mondal, Influence of Calcium Sulfoaluminate (CSA) Cement Content on Expansion and Hydration Behavior of Various Ordinary Portland Cement-CSA Blends, J. Am. Ceram. Soc. 8 (2015) n/a-n/a. doi:10.1111/jace.13645.

[35] P. Chaunsali, P. Mondal, Physico-chemical interaction between mineral admixtures and OPC-calcium sulfoaluminate (CSA) cements and its influence on early-age expansion, Cem. Concr. Res. 80 (2016) 10–20. doi:10.1016/j.cemconres.2015.11.003.

[36] D. Sirtoli, M. Wyrzykowski, F. Winnefeld, P. Riva, P. Lura, Volume changes of mortars based on calcium sulfoaluminate cement, Submitted to Cement and Concrete Research, 2019.

[37] M. Wyrzykowski, P. Lura, Effect of relative humidity decrease due to self-desiccation on the hydration kinetics of cement, Cem. Concr. Res. 85 (2016) 75–81. doi:10.1016/j.cemconres.2016.04.003.

[38] T.C. Powers, A Discussion of Cement Hydration in Relation to the Curing of Concrete, Highw. Res. Board Proc. 27 (1948) 178–188.

[39] O.M. Jensen, Thermodynamic limitation of self-desiccation, Cem. Concr. Res. 25 (1995) 157–164. doi:10.1016/0008-8846(94)00123-G.

[40] R.J. Flatt, G.W. Scherer, J.W. Bullard, Why alite stops hydrating below 80% relative humidity, Cem. Concr. Res. 41 (2011) 987–992. doi:10.1016/j.cemconres.2011.06.001.

[41] O. Coussy, Poromechanics, 2004. doi:10.1002/0470092718.

[42] H. Chen, M. Wyrzykowski, K. Scrivener, P. Lura, Prediction of self-desiccation in low water-to-cement ratio pastes based on pore structure evolution, Cem. Concr. Res. 49 (2013) 38–47.

625 doi:10.1016/j.cemconres.2013.03.013.
626 [43] Z. Hu, M. Wyrzykowski, K. Scrivener, P. Lura, A novel method to predict internal relative
627 humidity in cementitious materials by 1 H NMR, Cem. Concr. Res. (2017).
628 doi:10.1016/j.cemconres.2017.11.001.
629 [44] P. Lura, B. Lothenbach, Influence of Pore Solution Chemistry on Shrinkage of Cement Paste,
630 50-Year Teach. Res. Anniv. Prof. Sun Wei Adv. Civ. Eng. Mater. (2010) 191–200.
631 [45] I. Vlahinić, H.M. Jennings, J.J. Thomas, A constitutive model for drying of a partially saturated
632 porous material, Mech. Mater. 41 (2009) 319–328. doi:10.1016/j.mechmat.2008.10.011.
633 [46] O. Coussy, R. Eymard, T. Lassabatère, Constitutive Modeling of Unsaturated Drying
634 Deformable Materials, J. Eng. Mech. 124 (1998) 658–667. doi:10.1061/(ASCE)0733-
635 9399(1998)124:6(658).
636 [47] J.-M. Pereira, O. Coussy, E.E. Alonso, J. Vaunat, S. Olivella, Is the degree of saturation a good
637 candidate for Bishop's X parameter?, Alonso, E.E., Gens, A. Unsaturated Soils—Proceedings
638 5th Int. Conf. Unsaturated Soils. (2010) 913–919. doi:1010.2608.
639 [48] D. Sirtoli, S. Tortelli, M. Marchi, P. Lura, Drying and Autogenous Shrinkage Evolution of a
640 Blended CSA-Portland Cement Concrete, Spec. Publ. 326 (2018).
641 [49] G. Sant, B. Lothenbach, P. Juilland, G. Le Saout, J. Weiss, K. Scrivener, The origin of early
642 age expansions induced in cementitious materials containing shrinkage reducing admixtures,
643 Cem. Concr. Res. (2011). doi:10.1016/j.cemconres.2010.12.004.
644 [50] X. Li, Z.C. Grasley, E.J. Garboczi, J.W. Bullard, Modeling the apparent and intrinsic
645 viscoelastic relaxation of hydrating cement paste, Cem. Concr. Compos. 55 (2015) 322–330.
646 doi:10.1016/j.cemconcomp.2014.09.012.
647 [51] M. Wyrzykowski, K. Scrivener, P. Lura, Basic creep of cement paste at early age-the role of
648 cement hydration, Cem. Concr. Res. 116 (2019) 191–201.
649 [52] D.T. Nguyen, R. Alizadeh, J.J. Beaudoin, L. Raki, Microindentation creep of secondary
650 hydrated cement phases and C-S-H, Mater. Struct. Constr. (2013). doi:10.1617/s11527-012-
651 9993-0.
652 [53] Z.P. Bažant, M.H. Hubler, Q. Yu, Pervasiveness of excessive segmental bridge deflections:
653 Wake-up call for creep, ACI Struct. J. 108 (2011) 766–774.
654 doi:10.1017/CBO9781107415324.004.
655 [54] T.D. Lämmlein, F. Messina, M. Wyrzykowski, G.P. Terrasi, P. Lura, Low clinker high
656 performance concretes and their potential in CFRP prestressed structural elements, Cem.
657 Concr. Res. (2018).
658 [55] N. Neithalath, B. Pease, J.H. Moon, F. Rajabipour, J. Weiss, E. Attiogbe, Considering moisture
659 gradient and time-dependent crack growth in restrained concrete elements subjected to drying,

NSF Work. High Perform. Concr. (2005) 279–290.
[56] V. Gribniak, G. Kaklauskas, R. Kliukas, R. Jakubovskis, Shrinkage effect on short-term deformation behavior of reinforced concrete – When it should not be neglected, Mater. Des. 51 (2013) 1060–1070. doi:10.1016/j.matdes.2013.05.028.
[57] A. Bentur, Evaluation of early age cracking characteristics in cementitious systems, Mater. Struct. 36 (2003) 183–190. doi:10.1617/14014.
[58] P.-C. Aïtcin, High performance concrete, CRC press, 2011.
[59] O.M. Jensen, P. Lura, Techniques and materials for internal water curing of concrete, Mater. Struct. 39 (2006) 817–825. doi:10.1617/s11527-006-9136-6.
[60] P. Lura, O.M. Jensen, S.I. Igarashi, Experimental observation of internal water curing of concrete, Mater. Struct. Constr. 40 (2007) 211–220. doi:10.1617/s11527-006-9132-x.
[61] A.B. Hossain, J. Weiss, Assessing residual stress development and stress relaxation in restrained concrete ring specimens, Cem. Concr. Compos. 26 (2004) 531–540. doi:10.1016/S0958-9465(03)00069-6.
[62] A. Leemann, P. Lura, R. Loser, Shrinkage and creep of SCC - The influence of paste volume and binder composition, Constr. Build. Mater. 25 (2011) 2283–2289. doi:10.1016/j.conbuildmat.2010.11.019.
[63] H.S. Müller, I. Anders, R. Breiner, M. Vogel, Concrete: Treatment of types and properties in fib Model Code 2010, Struct. Concr. 14 (2013) 320–334. doi:10.1002/suco.201200048.
[64] G. Pickett, The effect of change in moisture-content on the creep of concrete under a sustained load, J. Am. Concr. Inst. 13 (1942) 333–355. doi:10.14359/8607.

## Appendix A – Technical documents formulation

For defining the shrinkage and creep functions according to the codes, the following aspects were considered. The measured average cubic compressive strength of each concrete was multiplied by 0.83 to transform it into an average cylindrical compressive strength $f_{cm}$. Other aspects defined for the model are the applied stress, which is one third of the compressive strength at the considered time of loading (25% for CPC), the relative humidity, which is that of the testing room (57% RH), the time of loading $t_0$, which takes into account the different loading steps (see section 2.5) and is adjusted by the room temperature of 20°C, the cement type, where a rapid hardening CEM I 42.5R is taken for all concrete mixtures (since no CSA cement is considered in the code), and the concrete age at the beginning of drying, set to 1 day.

A cement type III was considered in the ACI 209.R-92 model, as CEM I 42.5R is not included in that model. Moreover, only for the ACI 209.R-92 model, $f$ and $\alpha$ for the shrinkage prediction and $d$ and $\Psi$ for the creep prediction were taken as constant for a given member shape and size ($\alpha$ and $\Psi$ equal

to 1 for a flatter hyperbolic curve), all the composition parameters were referred to test values on fresh state just before the casting operation (slump, air content, volumetric mass) and as "fine aggregate" in the fine aggregate factor calculation the fraction below 3 mm was considered.

In the ACI 209.R-92 model, the creep was obtained in terms of creep coefficient. The subsequent extrapolation of the creep strain was obtained following the Model Code 2010 formulation in order to have similar references. The ACI 209.R-92 model considers as modulus of elasticity the one obtained according to the code based on the 28-days strength.

*Model Code 2010 - Creep strain*

$$\varepsilon_{cc}(t,t_0) = \frac{\sigma_c(t_0)}{E_{ci}} \cdot \varphi(t,t_0)$$

with

$$E_{ci} = E_{c0} \cdot \alpha_E \cdot \left(\frac{f_{cm}}{10}\right)^{1/3}$$

$$\varphi(t,t_0) = \varphi_{bc}(t,t_0) + \varphi_{dc}(t,t_0)$$

where

| | |
|---|---|
| $\varepsilon_{cc}(t,t_0)$ | creep strain at time $t > t_0$; |
| $\sigma_c(t_0)$ | applied constant stress at time $t_0$; |
| $E_{ci}$ | dynamic modulus of elasticity at age 28 days; |
| $\varphi(t,t_0)$ | creep coefficient; |
| $E_{c0}$ | assumed equal to $21.5 \cdot 10^3$; |
| $\alpha_E$ | constant, assumed to be 1 for quartzite aggregates; |
| $f_{cm}$ | mean compressive strength at age 28 days; |
| $\varphi_{bc}(t,t_0)$ | basic creep coefficient; |
| $\varphi_{dc}(t,t_0)$ | drying creep coefficient; |

*Model Code 2010 - Basic creep coefficient*

$$\varphi_{bc}(t,t_0) = \beta_{bc}(f_{cm}) \cdot \beta_{bc}(t,t_0)$$

with

$$\beta_{bc}(f_{cm}) = \frac{1.8}{(f_{cm})^{0.7}}$$

$$\beta_{bc}(t,t_0) = \ln\left[\left(\frac{30}{t_{0,adj}} + 0.035\right)^2 \cdot (t - t_0) + 1\right]$$

$$t_{0,adj} = t_{0,T} \cdot \left[\frac{9}{2 + t_{0,T}^{1.2}} + 1\right]^{\alpha} \geq 0.5\ days$$

$$t_{0,T} = \sum_{i=1}^{n} \Delta t_i \, exp\left[13.65 - \frac{4000}{273+T(\Delta t_i)}\right]$$

where

$t_{0,adj}$ modified age of loading, taking into account the type of cement and the temperature;

$\alpha$ coefficient that depends on the type of cement;

$t_{0,T}$ temperature-adjusted concrete age;

$\Delta t_i$ number of days where a temperature T prevails;

$T(\Delta t_i)$ temperature in °C during the time period $\Delta t_i$.

*Model Code 2010 - Drying creep coefficient*

$$\varphi_{dc}(t, t_0) = \beta_{dc}(f_{cm}) \cdot \beta(RH) \cdot \beta_{dc}(t_0) \cdot \beta_{dc}(t, t_0)$$

with

$$\beta_{dc}(f_{cm}) = \frac{412}{(f_{cm})^{1.4}}$$

$$\beta(RH) = \frac{1 - \frac{RH}{100}}{\sqrt[3]{0.1 \cdot \frac{h}{100}}}$$

$$h = \frac{2 \cdot A_C}{u}$$

$$\beta_{dc}(t_0) = \frac{1}{0.1 + \left(t_{0,adj}\right)^{0.2}}$$

$$\beta_{dc}(t, t_0) = \left[\frac{(t - t_0)}{\beta_h + (t - t_0)}\right]^{\gamma(t_0)}$$

$$\gamma(t_0) = \frac{1}{2.3 + \frac{3.5}{\sqrt{t_{0,adj}}}}$$

$$\beta_h = 1.5 \cdot h + 250 \cdot \alpha_{f_{cm}} \leq 1500 \cdot \alpha_{f_{cm}}$$

$$\alpha_{f_{cm}} = \left(\frac{35}{f_{cm}}\right)^{0.5}$$

where

*RH* relative humidity of the ambient environment in %;

*h* notional size of member, where $A_C$ is the cross-section in mm$^2$ and *u* is the perimeter of the member in contact with the atmosphere in mm.

*Model Code 2010 - Shrinkage*

$$\varepsilon_{cs}(t, t_s) = \varepsilon_{cas}(t) + \varepsilon_{cds}(t, t_s)$$

with

$$\varepsilon_{cas}(t) = \varepsilon_{cas0}(f_{cm}) \cdot \beta_{as}(t)$$

$$\varepsilon_{cas0}(f_{cm}) = -\alpha_{as}\left(\frac{f_{cm}/10}{6+f_{cm}/10}\right)^{2.5} \cdot 10^{-6}$$

$$\beta_{as}(t) = 1 - exp\left(-0.2 \cdot \sqrt{t}\right)$$

$$\varepsilon_{cds}(t, t_s) = \varepsilon_{cds0}(f_{cm}) \cdot \beta_{RH}(RH) \cdot \beta_{ds}(t - t_s)$$

$$\varepsilon_{cds0}(f_{cm}) = [(220 + 110 \cdot \alpha_{ds1}) \cdot exp(-\alpha_{ds2} \cdot f_{cm})] \cdot 10^{-6}$$

$$\beta_{RH}(RH) = f(x) = \begin{cases} -1.55 \cdot \left[1 - \left(\frac{RH}{100}\right)^3\right], & for\ 40 \le RH < 99\% \cdot \beta_{s1} \\ 0.25, & for\ RH \ge 99\% \cdot \beta_{s1} \end{cases}$$

$$\beta_{s1} = \left(\frac{35}{f_{cm}}\right)^{0.1} \le 1.0$$

$$\beta_{ds}(t - t_s) = \left[\frac{(t-t_s)}{0.035 \cdot h^2 + (t-t_s)}\right]^{0.5}$$

where

$\varepsilon_{cas}(t)$ autogenous shrinkage;

$\alpha_{as}$ coefficient dependent on the type of cement;

$\varepsilon_{cds}(t, t_s)$ drying shrinkage;

$\alpha_{ds1}, \alpha_{ds2}$ coefficients dependent on the type of cement;

$t_s$ concrete age at the beginning of drying, in days.

*ACI 209.R-92 - Creep strain*

$$\varepsilon_{cc}(t, t_0) = \frac{\sigma_c(t_0)}{E_{cmto}} \cdot \varphi(t, t_0)$$

with

$$E_{cmto} = 0.043 \cdot {\gamma_c}^{1.5} \cdot \sqrt{f_{cmt0}}$$

$$f_{cmt0} = \left[\frac{t}{a+bt}\right] \cdot f_{cm28}$$

$$\varphi(t, t_0) = \frac{(t - t_0)^{\Psi}}{d + (t - t_0)^{\Psi}} \cdot \varphi_u$$

$$d = 4 \cdot \frac{V}{S}$$

$$\varphi_u = 2.35 \cdot \gamma_c$$

$$\gamma_c = \gamma_{c,t0} \cdot \gamma_{c,RH} \cdot \gamma_{c,vs} \cdot \gamma_{c,s} \cdot \gamma_{c,\Psi} \cdot \gamma_{c,\alpha}$$

$$\gamma_{c,t0} = 1.25 \cdot {t_0}^{-0.118} \quad \text{for moist curing}$$

$$\gamma_{c,RH} = 1.27 - 0.67 \cdot h \quad \text{for } h \ge 0.40$$

$$\gamma_{c,vs} = \frac{2}{3} \cdot \left(1 + 1.13 \cdot e^{\{-0.0213(V/S)\}}\right) \quad \text{in SI units}$$

$$\gamma_{c,s} = 0.82 + 0.00264 \cdot s \quad \text{in SI units}$$

$$\gamma_{c,\Psi} = 0.88 + 0.0024 \cdot \Psi$$

$$\gamma_{c,\alpha} = 0.46 + 0.09 \cdot \alpha \geq 1$$

where

| | |
|---|---|
| $\varepsilon_{cc}(t, t_0)$ | creep strain at time $t > t_0$; |
| $\sigma_c(t_0)$ | applied constant stress at time $t_0$; |
| $E_{cmt0}$ | modulus of elasticity at time $t_0$; |
| $\varphi(t, t_0)$ | creep coefficient; |
| $\gamma_c$ | unit weight of concrete; |
| $f_{cmt0}$ | mean compressive strength at time $t_0$; |
| $a, b$ | constants referred to a moist cured type III cement; |
| $d, \Psi$ | constant for a given member shape and size; |
| $\varphi_u$ | ultimate creep coefficient; |
| $\gamma_c$ | cumulative product of the applicable correction factors; |
| $\gamma_{c,t0}$ | age of loading factor; |
| $\gamma_{c,RH}$ | ambient relative humidity factor; |
| $\gamma_{c,vs}$ | size of member factor; |
| $\gamma_{c,s}$ | slump factor; |
| $\gamma_{c,\Psi}$ | fine aggregate factor; |
| $\gamma_{c,\alpha}$ | air content factor. |

*ACI 209.R-92 - Shrinkage*

$$\varepsilon_{sh}(t, t_c) = \frac{(t - t_c)^{\alpha}}{f + (t - t_c)^{\alpha}} \cdot \varepsilon_{shu}$$

$$f = 26 \cdot e^{\left\{1.42 \times 10^{-2}\left(\frac{V}{S}\right)\right\}} \quad \text{in SI units}$$

$$\varepsilon_{shu} = 780 \cdot \gamma_{sh} \times 10^{-6}\ [mm/mm]$$

$$\gamma_{sh} = \gamma_{sh,tc} \cdot \gamma_{sh,RH} \cdot \gamma_{sh,vs} \cdot \gamma_{sh,s} \cdot \gamma_{sh,\Psi} \cdot \gamma_{sh,c} \cdot \gamma_{sh,\alpha}$$

$$\gamma_{sh,tc} = 1.202 - 0.2337 \cdot \log(t_c)$$

$$\gamma_{sh,RH} = \begin{cases} 1.40 - 1.02 \cdot h, & for\ 0.40 \leq h < 0.80 \\ 3.00 - 3.0 \cdot h, & for\ 0.80 \leq h < 1 \end{cases}$$

$$\gamma_{sh,vs} = 1.2 \cdot e^{\{-0.00472(V/S)\}} \quad \text{in SI units}$$

$$\gamma_{sh,s} = 0.89 + 0.00161 \cdot s \quad \text{in SI units}$$

$$\gamma_{sh,\Psi} = \begin{cases} 0.30 + 0.014 \cdot \Psi, & for\ \Psi \leq 50\% \\ 0.90 + 0.002 \cdot \Psi, & for\ \Psi > 50\% \end{cases}$$

$$\gamma_{sh,c} = 0.75 + 0.00061 \cdot \mathrm{c} \quad \text{in SI units}$$

$$\gamma_{sh,\alpha} = 0.95 + 0.008 \cdot \alpha \geq 1$$

where

| | |
|---|---|
| $\varepsilon_{sh}(t, t_c)$ | shrinkage strain at time $t > t_c$; |
| $f, \alpha$ | constants depending on member shape and size; |
| $\varepsilon_{shu}$ | ultimate shrinkage strain; |
| $\gamma_{sh}$ | cumulative product of the applicable correction factors; |
| $\gamma_{sh,t0}$ | age of loading factor; |
| $\gamma_{sh,RH}$ | ambient relative humidity factor; |
| $\gamma_{sh,vs}$ | size of the member factor; |
| $\gamma_{sh,s}$ | slump factor; |
| $\gamma_{sh,\Psi}$ | fine aggregate factor; |
| $\gamma_{sh,c}$ | cement content factor; |
| $\gamma_{sh,\alpha}$ | air content factor. |